THE NASA TETRAHEDRAL UNSTRUCTURED SOFTWARE SYSTEM (TETRUSS)

Neal T. Frink, Shahyar Z. Pirzadeh, Paresh C. Parikh
NASA Langley Research Center
Hampton, Virginia, U.S.A.

Mohagna J. Pandya, M. K. Bhat
Paragon Research Inc.
Hampton, Virginia, U.S.A.

Keywords: *unstructured, tetrahedral, Navier-Stokes, aeroelastic, design*

Abstact

The NASA Tetrahedral Unstructured Software System (TetrUSS) was developed during the 1990's to provide a rapid aerodynamic analysis and design capability to applied aerodynamicists. The system is comprised of loosely integrated, user-friendly software that enables the application of advanced Euler and Navier-Stokes tetrahedral finite volume technology to complex aerodynamic problems. TetrUSS has matured well because of the generous feedback from many willing users representing a broad cross-section of background and skill levels. This paper presents an overview of the current capabilities of the TetrUSS system along with some representative results from selected applications.

1 Introduction

The last decade of the twentieth century brought about remarkable progress in practical computational aerodynamic analysis and design capability. This phenomenon was largely fueled by breakthrough developments in the science of Computational Fluid Dynamics (CFD), geometric modeling, computer architecture, and networking speeds. Intense competitive pressures to build more efficient or specialized products, e.g. aircraft, automobiles, buildings, pumps, heat exchangers, etc., in less time and at lower cost and risk, further drove demand for more timely solutions to fluid dynamic problems. Consequently, CFD tools are now a critical component of many design processes that, in the past, relied solely on empirical and experimental techniques.

The underlying methodologies for CFD have evolved over the past 30 years through the efforts of many talented researchers. The majority of work has centered on the *structured*-grid approach for solving the Euler and Navier-Stokes flow equations, where discretization of space is accomplished by hexahedral volume elements. The natural ordering of hexahedral cells enables the construction of very efficient numerical algorithms for solving the flow equations. While amenable to algorithmic efficiency, *structured*-grids are inherently difficult to construct around complex geometries. Innovative remedies were devised for decomposing the global grid into simpler component grids that could be generated more readily. Communication between component grids is achieved either by direct transfer across interfacing boundaries (patched grids), or by interpolation within overlapping grid regions (overset grids). These extensions are responsible for the continued success of the *structured*-grid codes today, particularly for commercial transport aircraft companies where the underlying configuration has changed very little over time.

For more complex and unconventional geometries, *structured* grid generation times routinely extend into weeks or months. Because of the growing demand for more timely application of CFD tools to increasingly complex and unique problems, researchers began during the mid- to late-1980's to explore the *unstructured*-grid approach using triangular elements in two dimensions and tetrahedral cells in three-dimensions. These elements had been used in the finite-element structural analysis community for many years, and were known to be exceptionally adaptable for discretizing complex shapes. While several *unstructured*-grid methodologies have realized considerable success in recent years, their underlying algorithms are still relatively new and diverse. There are still many philosophical differences among researchers regarding the superiority of one approach over another. A good overview of the technology is presented in Ref. [1].

Some of the most enabling advancements toward rapid CFD application have occurred in the area of tetrahedral grid generation [2-6]. With the advent of the Advancing Front Method [2] and the Advancing-Layers Method [3], 'viscous' tetrahedral grids can now be generated on complex, full aircraft configurations within days.

With the recent advancements in *unstructured* CFD technology, a tremendous benefit is gained by harnessing the various component technologies into a user-friendly system. The NASA *Tetra*hedral *U*nstructured *S*oftware *S*ystem (*TetrUSS*) was developed at NASA Langley Research Center during the 1990's to address this need. *TetrUSS* is a loosely integrated *unstructured-grid* based CFD system that provides ready access to rapid, higher-order analysis and design capability for the applied aerodynamicist. From a developer's perspective, the maturation of the underlying methodology is greatly accelerated by encouraging feedback from user applications of the system to focused problems. While specific codes are currently used within the *TetrUSS* system, it is sufficiently modular such that other component

codes can be easily interchanged if desired. The primary value of the present work stems from the engineering capability derived by the integration of state-of-the-art CFD technologies.

2 Overview of Current Capability

The *TetrUSS* system, illustrated in Fig. 1, consists of component software for setting up geometric surface definitions, generating discrete computational grids, computing Euler and/or Navier-Stokes flow solutions, imposing design or aeroelastic shape changes, and extracting meaningful information for analysis of the results. The primary component codes within the *TetrUSS* system are denoted in Fig. 1 as GridTool, VGRIDns, USM3Dns, and VIGPLOT. However, as evidenced by several other codes included within parenthesis, the system is sufficiently flexible that other researchers have also benefited by replacing various components with their own codes. The capabilities of the current system are described in the following subsections.

2.1 Grid Generation

2.1.1 GridTool
GridTool [7] is an interactive program for grid/geometry applications which bridges the gap between Computer Aided Design (CAD) representations and grid generation systems. It supports many useful functions for modifying or
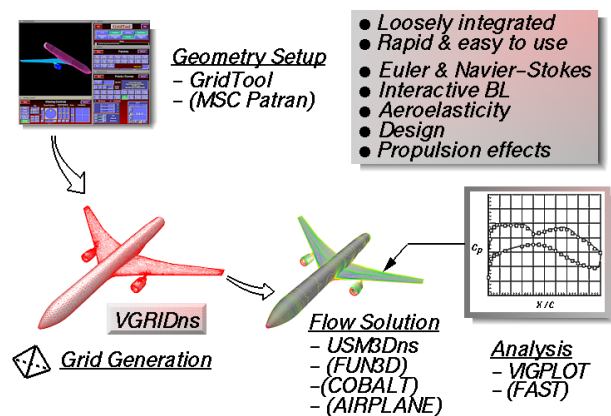

Fig. 1 The Tetrahedral Unstructured Software System (*TetrUSS*).

repairing surface definitions, as well as for preparing an input file for VGRIDns. While several file formats are readable by the software, the Initial Graphics Exchange Specifications (IGES) format [8] is most widely used as an interface between CAD and GridTool.

2.1.2   VGRIDns/POSTGRID

VGRIDns is a computer program for automatic generation of tetrahedral unstructured grids suitable for computing Euler and Navier-Stokes flow solutions. The methodology is based on the Advancing-Front method (AFM) [2] and the Advancing-Layers method (ALM) [3]. Both techniques are based on marching processes in which tetrahedral cells grow on an initial front (triangular boundary mesh) and gradually accumulate in the field around the subject geometry. Unlike the conventional AFM, which introduces cells in the field in a totally unstructured manner, the ALM generates layers of thin tetrahedral cells in a more orderly fashion (one layer at a time) while maintaining the flexibility of the AFM. Once the advancing front process is completed in VGRIDns, an additional postprocessing step is required using POSTGRID to close any open pockets and to improve grid quality.

The input data file to VGRIDns is set up in GridTool. A number of contiguous surface patches are constructed over the underlying IGES surface definition. The grid characteristics such as spacing and stretching parameters, rate of growth, etc. are also prescribed by the user with GridTool to complete the input data file. The process of geometry and grid parameter preparation with GridTool constitutes 50-90% of the total grid-generation time depending on the complexity of the geometry and the "cleanliness" of the surface definition.

Cartesian background grid - Information regarding the unstructured grid point distribution is provided to the AFM and ALM marching processes by a "transparent" Cartesian background grid overlaying the entire domain [9]. Included in the background grid are a number of "point" and "line" sources prescribed

by the user. The sources contain information about the characteristics of the final unstructured grid to be generated. The information is first distributed smoothly from the sources onto the background grid nodes by solving a Poisson equation. The problem is similar to that of the heat transfer in a conducting medium. The smoothed parameters are then interpolated from the background grid (and sources) to the unstructured grid points being generated on the surface and in the field during the marching processes.

Thin-layer Navier-Stokes grid generation - The thin-layered tetrahedral cells required for Navier-Stokes solutions are generated by the ALM method [3]. Points are distributed along predetermined direction vectors according to a user-prescribed stretching function. Cell-to-node connectivity is dictated by a predetermined connectivity pattern. The layers grow into the field until some limiting criteria, based on the background grid information and/or proximity of the approaching fronts, prevent the layers from further advancement. At this point, the process automatically switches from the ALM to the AFM mode to generate regular grid outside the boundary layer. With a common background grid controlling both methods, the transition from thin layers to the regular grid becomes gradual and continuous. In addition, the fact that the number of layers varies from one location to another adds to the flexibility of the method and the smoothness of the generated grids.

Multidirectional anisotropic cell stretching A salient feature of VGRIDns is its ability to generate multi-directional, anisotropic stretched grids in which the surface triangles and tetrahedra in the field are elongated in user-prescribed directions [10]. With this capability, fewer points are distributed in the directions of reduced flow gradient without loss of grid resolution in other essential directions. Grid stretching is achieved by prescribing a stretching direction and two spacing factors (along and normal to the stretching direction) for each background grid source. Anisotropic stretching

is a powerful tool for generating efficient unstructured grids. Application of this option to a typical aircraft configuration results in reduction of grid size at least by a factor of three.

2.1.3   Grid Movement

Grid movement capability is utilized for problems such as time-dependent flows involving moving bodies, aeroelastic analysis of aircraft undergoing surface deflections, interactive CFD/design analysis resulting in geometry perturbation, etc. An unstructured grid movement method has been developed in this work to perturb tetrahedral volume grids according to the movement or deformation of the subject geometries [3]. The method is based on a "spring" analogy for moving inviscid grids, and a combination of spring and "surface vector readjustment" methods for moving thin-layer Navier-Stokes grids. The scheme is very robust for moving thin layers of viscous grids. As long as the fidelity of the surface definition is preserved after perturbation, it always produces a valid grid.

2.2   Flow Solver

2.2.1   USM3Dns Salient Features

USM3Dns [11,12] is a tetrahedral cell-centered, finite volume Euler and Navier-Stokes (N-S) flow solver. Inviscid flux quantities are computed across each cell face using Roe's [13] flux-difference splitting (FDS). Spatial discretization is accomplished by a novel reconstruction process [14], which is based on an analytical formulation for computing solution gradients within tetrahedral cells. The solution is advanced to a steady state condition by an implicit backward-Euler time-stepping scheme [15]. Flow turbulence effects are modeled by the Spalart-Allmaras (S-A) one-equation model [16], which is coupled with a wall function to reduce the number of cells in the sublayer region of the boundary layer.

USM3Dns runs with multitasking on Cray vector processors, and more recently on massively parallel processors. Memory is allocated dynamically. The code requires 175 eight-bit words per tetrahedra, and runs with individual processor times of 34 μsec/cell/cycle on a Cray-C90 and 230 μsec/cell/cycle on a single CPU of an Origin 2000. Work is underway to port the parallel code to personal computer (PC) clusters.

2.2.2   Boundary conditions

The USM3Dns code is designed for the easy addition/modification of boundary conditions (B.C.). It supports the standard B.C.'s of flow tangency or no-slip on solid surfaces, characteristic inflow/outflow for subsonic boundaries, and freestream inflow and extrapolation outflow for supersonic flow. Some additional special boundary conditions are available as well.

Wall Function - The S-A model has been coupled with a wall function formulation to reduce the need for grid resolving the flow in the sublayer portion of a turbulent boundary layer. With this approach, the inner region of the boundary layer is modeled by an analytical function that is matched with the numerical solution in the outer region. The wall function formulation has the advantage of 1) significantly reducing the memory requirement by eliminating a large portion of cells normally required to resolve the sub-layer, and 2) improving overall convergence by removing the thinner, more highly stretched cells which add stiffness to the solution process. More details are presented in Ref. [12].

Wake flow –VGRIDns does not presently support the generation of thin-layered tetrahedral field cells for resolving the wake flow behind a wing trailing edge (TE). Thus, it is difficult to enforce adequate grid resolution downstream of the TE without resorting to excessive numbers of cells. A special B.C. [17] has been developed to mimic the relieving effect of a blunt-base wake on a coarse grid, which is useful for cases where the wing has a thick TE. The approach is to introduce a *solution-defined* transpiration velocity on the blunt-base boundary faces to provide a smooth departure of

the flow past the corner. This B.C. has been tested and is used extensively with inviscid flows and wall function applications.

Jet-engine – USM3Dns supports a B.C. for modeling propulsion-induced effects of up to four turbofan, turbojet, or jet-nozzle components. The model [18] computes inflow and/or outflow B.C.'s from user prescribed values for the total pressure and temperature change across or within the combustor, the exit pressure, the fuel fraction, and the direction cosines for the jet exit. The inlet mass flow is automatically balanced with that of the nozzle.

Propeller – A propeller/rotor B.C. has been constructed based on an actuator disk model [19]. Since VGRIDns does not presently support a capability to generate volume grids around 'zero-thickness' surfaces by itself, a novel procedure has been developed for this purpose. The procedure provides necessary pre- and post-processing utilities for VGRIDns to generate volume grids around a zero-thickness rotor. The rotor is composed of two distinct discretized surfaces, designated as rotor front (pointing towards the incoming flow to the rotor) and rotor back (pointing in opposite direction to rotor front) respectively, which are collapsed onto each other. In USM3Dns, a subsonic exit flow boundary condition has been imposed on the rotor front surface whereas a subsonic inlet boundary condition has been imposed on the rotor back while enforcing mass conservation. These boundary conditions are computed based on the rotor properties provided by a user input. The properties include thrust, torque, direction of rotation, size and location of each of the rotors/propellers. Provision has been made so that a user can simulate a uniform or radially varying pressure and/or swirl. Up to four independent rotors can be simulated in a single computational domain.

2.2.3 Parallel Processing.

The USM3Dns flow solver has been parallelized for efficient operation on both shared memory systems and a cluster of UNIX workstations connected by a local area network [20]. The

tetrahedral grid must be partitioned into a user specified number of contiguous zones with an approximately equal number of cells. Grid partitioning is accomplished by a mathematically rigorous "spectral bifurcation" graph partitioning technique called Metis [21] that has been adapted to the *TetrUSS* system.

Communication between partitions is accomplished through Message Passing Interface (MPI) calls embedded into the solver. Efficiency is achieved through an innovative use of specialized data structures, send and receive arrays, non-blocking communication, and "cache-friendly" local renumbering of cells in a partition.

The efficiency of the parallelized solver is demonstrated on the Numerical Aerodynamic Simulator (NAS) Origin 2000 computer using a generic business-jet configuration in Fig. 2. The geometry is comprised of a fuselage, a wing, and an engine nacelle mounted on the rear of the fuselage. The global grid contains 1,610,507 tetrahedral cells, and resolves the boundary layer with a y^+=50 using the wall function. The flow conditions are M_∞=0.85 and Re_{cref}=3 million. Each case was run for 1500 cycles.

A super-linear increase in speed relative to the ideal scaled level is observed in Fig. 2 for up to 200 processors. The speed-up efficiencies are referenced to a 10-processor solution, which was the minimum number of processors on
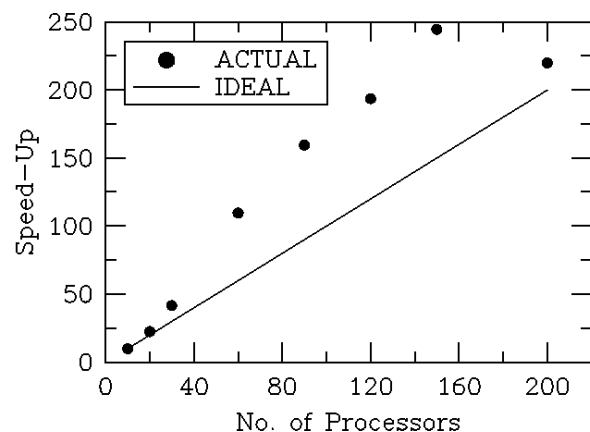

Fig. 2 Efficiency of USM3Dns parallel flow solver on Origin 2000 for a generic business-jet configuration.

which a partitioned grid of this size would fit into processor memories. It is assumed that a 10-processor solution gives a ten-fold increase in speed as compared to a single-processor solution. The super-linear performance is attributed to an increased cache efficiency resulting from an increasingly larger fraction of cells of any given partition fitting into cache memory of a processor. The reduced efficiency at 200 processors illustrates the potential of under filling the cache with smaller partitions such that the overhead from inter-zonal communication overrides the earlier benefits realized from cache efficiency.

It is important to note that the solution histories were essentially identical for any number of processors. Thus, the speed benefits realized in Fig. 2 come with no penalty in accuracy or global convergence.

2.2.4 *Low-Mach Preconditioning*

The flow analysis capability of USM3D has been extended for the low-speed flow regime by implementing a local preconditioning approach [22]. A preconditioner matrix of Weiss-Smith [23] has been used to pre-multiply the time derivatives of the governing equations such that a well-conditioned system of eigenvalues is rendered at low speeds. Applications with the code have demonstrated convergence behavior and solution quality that is nearly independent of the Mach number. The low-Mach preconditioning capability is currently available only in the serial version of USM3Dns.

2.3 Modular Engineering Capabilities

TetrUSS includes a modular capability [24] for computing aeroelastic effects [25], iterative design [26], and/or interactive boundary layer [27]. Each component, illustrated in Fig. 3, is maintained independently and is coupled to the system by pre- and post-processing utilities. The capabilities can all be used simultaneously, or in any combination.

During the script-driven update cycle, a solution file is written by the flow solver and is used along with the grid file by the sub-modules. Both the aeroelastic and design features involve grid movement, whereas the interactive boundary layer (IBL) feature generates transpiration boundary condition velocities.

The aeroelastic component converts the loads from the flow file into input for the structural code. The present options for structural modeling include a coupling with the ELAPS code [28] and the ENSAERO system [29]. The ELAPS code is a computationally efficient method based on plate model to solve for a polynomial global displacement function using the Rayleigh-Ritz method. Higher-level Finite Element Model (FEM) structural representations can be input through ENSAERO via modal or stiffness matrices.

The iterative design capability is provided by the Constrained Direct Iterative Surface Curvature (CDISC) method [26]. CDISC uses a knowledge-based approach to modify target pressure distributions that are used by the underlying DISC method to match flow constraints. The basic DISC design method is an iterative approach to modifying an aerodynamic surface to obtain a given surface pressure distribution. It is based on analytically derived expressions relating changes in surface curvature to a change in surface pressure coefficient, or more recently surface Mach number. Since this relationship is known apriori, the design can be converged very efficiently in parallel with the flow solution.
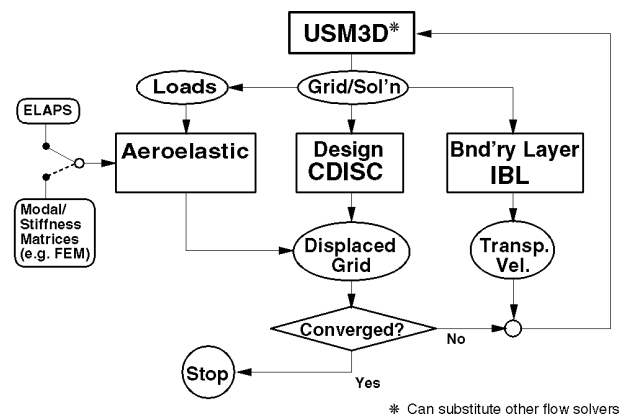

Fig. 3 Schematic of modular *TetrUSS* system

Two 2D boundary layer modules are currently available. The first is a proprietary code based on the inverse boundary layer methodology of Cebeci, et. al. [30]. In this method, the boundary layer is solved iteratively as part of the 2D boundary layer solution. Using the boundary layer edge values, the surface transpiration velocities are calculated, which in turn, are used as a boundary condition by the inviscid flow solver, thus indirectly accounting for the boundary layer displacement thickness.

The second module is in the public domain, and uses the Green's Lag Entrainment method [31]. This method employs the momentum integral equation, the entrainment equation and an equation for the streamwise rate of change of entrainment coefficient to calculate turbulent boundary layer characteristics.

Examples of the IBL and static aeroelastic capabilities will be shown in section 3.2.

2.4 Graphic Postprocessing

VIGPLOT [32] is an interactive, menu-driven post-processing program for extraction and display of data on unstructured (tetrahedral) grids. It displays grids and flow quantities on either boundary or user defined arbitrary planes in the field. Flow quantities can be displayed using line or filled contours, velocity vectors and particle traces. Some unique features include dynamic memory allocation, a 'probe' option that lets a user query the local value of a certain displayed fluid dynamic quantity, ability to plot two different sets side-by-side and a journaling (log file) capability. Grid post-processing options allow a user to isolate and display 'bad' grid cells and to visually confirm boundary conditions before proceeding with the flow solution. Several hardcopy output options are available.

Other graphic postprocessors can also be used with *TetrUSS*. Output files are supported for the well-known FAST and Tecplot codes.

2.5 Utility Codes

Several useful utility codes are maintained through a common interface called "usgutil". They are:
1. USM3Dns to Tecplot converter,
2. Mirroring of grid or VGRIDns input file,
3. Extracting cross-sectional or field data for density, velocity, energy, pressure, pressure coefficient (Cp), Mach number, temperature, entropy, or total pressure, and,
4. Providing an estimate for grid spacing and stretching parameters used in VGRIDns for viscous grids.

3 Selected Applications

An assessment of the *TetrUSS* technology is made using selected examples that emphasize various features. Two 2D flat-plate cases are presented to address solution accuracy for laminar and turbulent flows. Five 3D simulations are shown to assess 1) Euler/IBL coupled with aeroelasticity on a generic transonic transport wing/body configuration, 2) N-S subsonic laminar vortical flow, 3) N-S transonic separated flow on an unconventional aircraft, 4) Euler and N-S comparison on a complex fighter configuration, and 5) N-S supersonic flow with coupled aeroelasticity on supersonic transport configuration. The Spalart-Allmaras turbulence model is used in conjunction with the wall function for all turbulent N-S computations.

3.1 2D Test Cases

3.1.1 *Laminar Flat-Plate Boundary Layer*

A laminar Navier-Stokes USM3Dns solution is computed on a flat plate for comparison with the exact Blasius boundary layer solution to validate the numerical treatment of the viscous stencil. A quasi-2D "channel" grid was constructed by subdividing each hexahedral cell of a 49×41×3 *structured* grid into six tetrahedral cells. The

resulting *unstructured* grid has 23040 tetrahedral cells.

The flow solution was computed at $M_\infty=0.5$ and a $Re_L=10000$. A comparison of the velocity profiles is shown in Fig. 4 for several chord stations. The transformed computed profiles collapse well between longitudinal stations 0.20L and 0.95L, and are in good agreement with the exact Blasius solution.

3.1.2 Turbulent Flat-Plate Boundary Layer

A flat plate turbulent boundary-layer solution at $M_\infty=0.5$ and $Re_L=2$ million is used to assess the accuracy of the wall function in predicting turbulent skin friction. A second quasi-2D "channel" grid, similar to that for the laminar case, was constructed from a 49×19×3 hexahedral grid. The final *unstructured* grid contains 10368 tetrahedral cells. The initial normal spacing yields a $y^+=80$ at x/L=0.5.

Fig. 5 reveals very good agreement between the computed and theoretical skin friction coefficient, C_f. More details are presented for similar comparisons in Ref. [12].

3.2 3D Test Cases

3.2.1 NTF Pathfinder I – Euler with IBL and aeroelasticity

The transonic aerodynamics of transport configurations with supercritical airfoils can present a formidable challenge to predict computationally. Not only are the viscous effects important, but also the load-induced deformation of the thin high-aspect ratio wings experienced during wind-tunnel testing and flight. The location of the transonic shock is extremely sensitive to both factors. Thus, viscous and static aeroelastic effects must be accounted for in order to achieve a meaningful correlation for this class of vehicle.

The modular *TetrUSS* system has been applied to the National Transonic Facility (NTF) Pathfinder I wing/body configuration at a transonic, high Reynolds number flow condition [25]. Viscous effects are estimated from a coupled Euler/IBL solution, and static aeroelastic effects from a simple plate
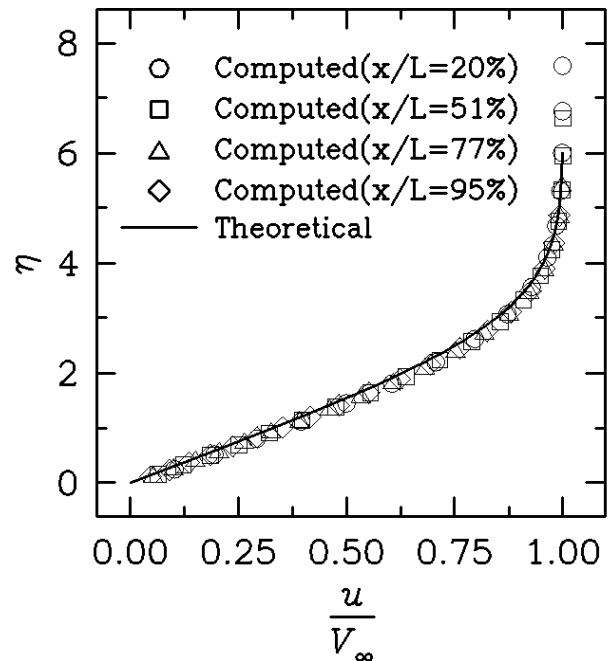

Fig. 4 Comparison of exact Blasius solution for laminar flow over flat plate with USM3Dns result. $M_\infty=0.5$, $Re_L=10000$.
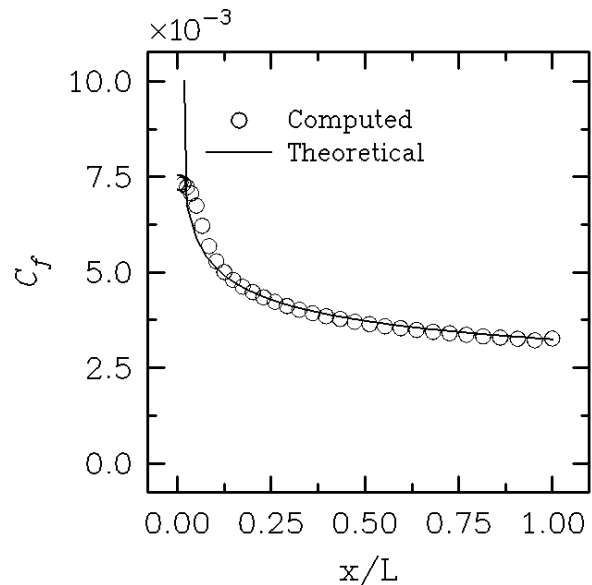

Fig. 5 Comparison of computed vs. theoretical skin friction coefficient for turbulent flat-plate flow. $M_\infty=0.5$, $Re_L=2$ million.

representation constructed for the ELAPS code. An additional single-point calibration has been made to the ELAPS model using static bending data measured on the wind-tunnel model. The
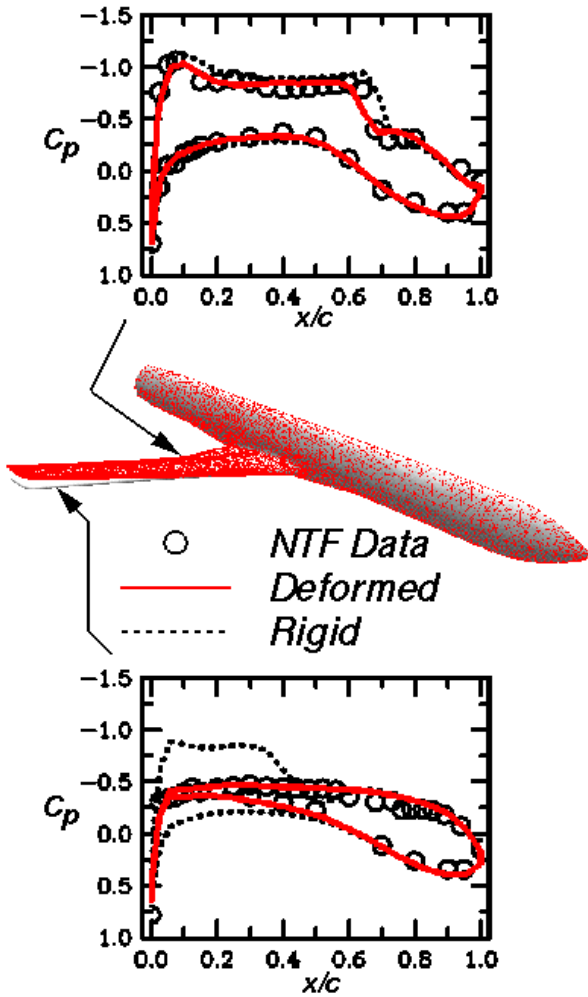
Fig. 6 Effect of aeroelastic deformation on Cp correlation for NTF Pathfinder I wing/body configuration at a transonic, high Reynolds number flow condition

Fig. 7 Comparison of computed and experimental surface pressure data and surface triangulation and "oil-flow" patterns. M_∞=0.3, α=20.5 deg., and Re_{cref}=900,000.

strength of this approach is that, with a single-point pretest calibration of a simple structural representation, the static aeroelastic effects can be accounted for in CFD calculations across a range of test conditions. No prior knowledge of the model deformation during the wind-on test is required.

Fig. 6 depicts a comparison of the rigid and deformed Pathfinder solutions with experimental pressure data at two span stations. The deformed solution is converged from the rigid geometry after 25 iterations through the modular system. Ten flow cycles were performed between each grid deformation. This result confirms that the accounting for static aeroelastic effects is critical to a good
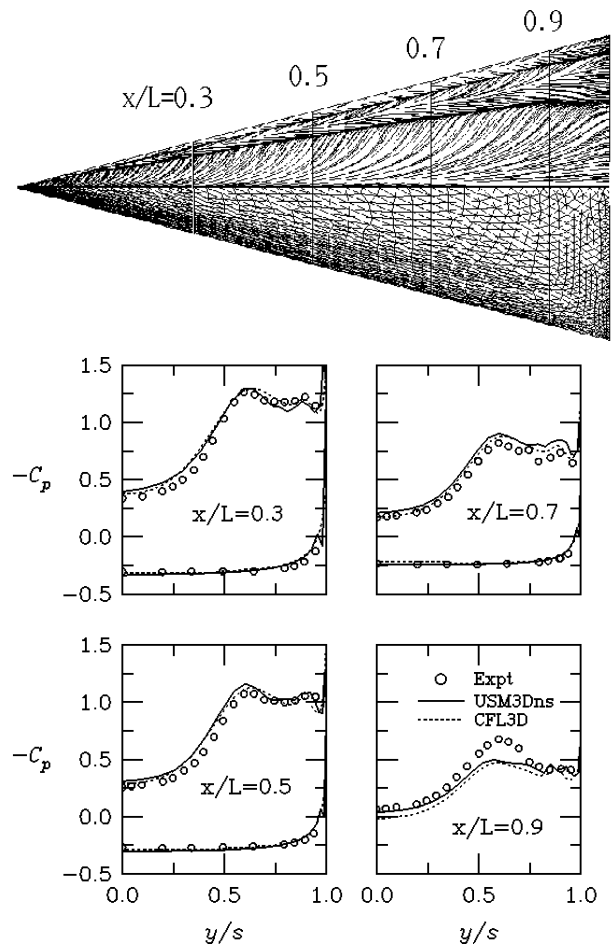
correlation with the data for this class of vehicle.

3.2.2 *Hummel Delta Wing – N-S, Subsonic, Laminar Vortical Flow*

A laminar Navier-Stokes flow solution was computed on the aspect-ratio 1 delta wing tested by Hummel [33]. Flow conditions were M_∞=0.3, α= 20.5 deg., and Re_{cref}=900,000. A grid of 730,454 tetrahedra was generated with normal spacing distributed near the surface to yield approximately 10 nodes (30 tetrahedra) in the mid-chord boundary layer for laminar flow. Anisotropic stretching, evident in the surface grid shown in Fig. 7, is utilized to reduce the chordwise density cells in the grid. This resulted

in a 7-fold reduction in grid size compared to standard isotropic triangles. A companion structured-grid computation was performed with the well-established CFL3D code [34] on a $65 \times 65 \times 33$ (span-radial-chordwise) H-O grid for comparison.

Fig. 7 portrays the surface "oil-flow" pattern and a comparison of the spanwise distribution of pressure coefficient, C_p, at four chord stations. The coalescing and diverging streamlines in the computed flow patterns show evidence of the primary, secondary, and tertiary vortices. Good agreement is noted between the *unstructured* and *structured* solutions, and with the experimental data of Hummel.

3.2.3 *Joined Wing – N-S, Transonic, Separated Flow*

A computation was made on the Joined-Wing configuration published in Ref. [35] in order to calibrate USM3Dns on an unconventional aircraft configuration operating at transonic, separated flow conditions. A thin-layered tetrahedral grid of 1,400,984 cells (246,891 nodes) was generated on the half-configuration. Grid size is kept small by utilizing anisotropic cell stretching which results in a factor-of-three fewer cells than an isotropic grid with similar chordwise resolution. The normal grid spacing was sized for wall function to yield a nominal midchord y^+=50 for the first node above the

surface and 18 to 20 tetrahedra across the boundary layer. The grid was completed in three days.

Fig. 8 depicts the surface triangulation and representative "oilflow" patterns on the joined-wing configuration. Significant shock-induced and trailing-edge flow separations are observed on the fore and aft wings. Severe flow reversal is evident on the tip panel. The surface flow patterns are in good agreement with experimental oilflow data (not shown) obtained in the NASA Langley Research Center 16-Foot Transonic Tunnel.

Fig. 9 portrays the longitudinal pressure coefficient (C_p) distribution along three representative spanwise stations of the fore and aft wings, and tip panel. The computed pressures are in good agreement in each flow region with the experimental data. The computation required 250MW of memory and 27 CPU hours on a CRAY C90. With multitasking on 10 processors, the solution was completed in 5 wall-clock hours.

3.2.4 *F-16 Aircraft with Stores – N-S and Euler*

Unstructured transonic Navier-Stokes computations are presented from Ref. [36] for the complete F-16 aircraft configuration in an ongoing assessment of *TetrUSS* for aerodynamic analysis of very complex geometries and flow
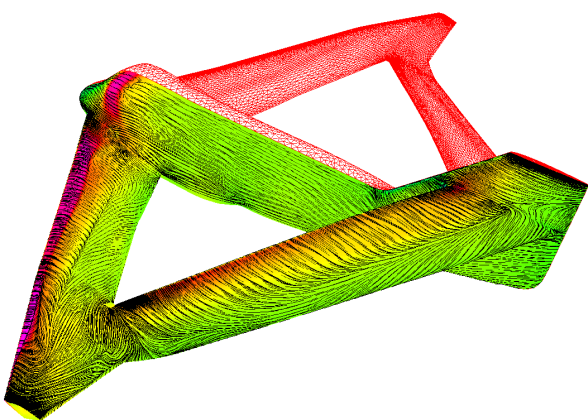

Fig. 8 Surface triangulation and "oilflow" patterns for a joined-wing configuration. magenta = low pressure and green = high pressure.
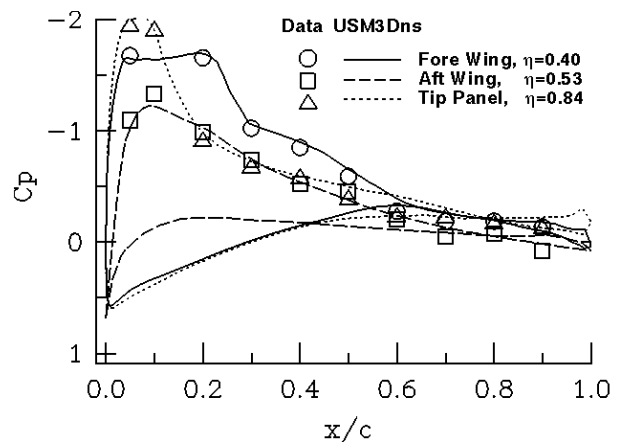

Fig. 9 Comparison of Cp distributions for joined-wing configuration on forward and aft wings, and tip panel at transonic Mach number and wind-tunnel Reynolds number.
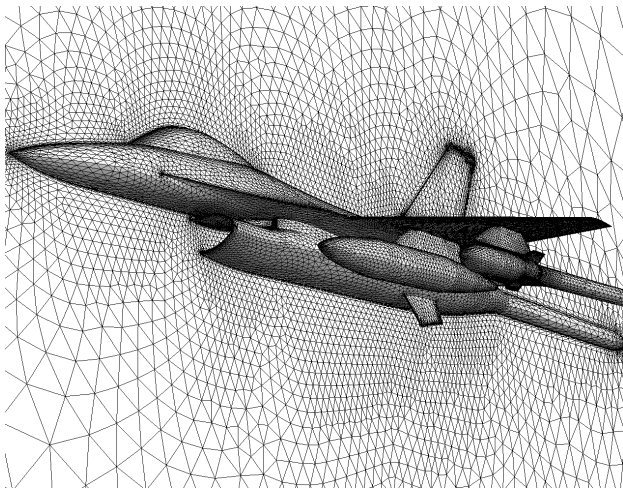
Fig. 10 Viscous tetrahedral grid on complete F-16 aircraft with external stores, 1,428,779 cells. Note thin-layer clustering on symmetry plane.

fields. A thin-layered tetrahedral grid of 1,428,779 cells (255,959 nodes) was generated for a full F-16 aircraft configuration with VGRIDns (see Fig. 10). A companion "inviscid" grid of 1,111,762 cells (not shown) was also generated for comparison purposes. Grid sizes were kept small by utilizing anisotropic cell stretching. The initial viscous grid was completed within approximately 40 to 60 hours of labor.

Turbulent flow solutions were computed with the USM3Dns flow solver at angles of attack (α) of 0, 2, 4, and 8 degrees, M_∞=0.95, and Re_{cref}=2 million based on mean aerodynamic chord. The normal grid spacing was sized for the wall function to yield a nominal midchord y^+=30 for the first node above the surface and 18 to 20 tetrahedra across the boundary layer.

Fig. 11 compares the longitudinal distribution of C_p from Euler, N-S, and experimental data along the inboard and outboard sides of the outer 'finned' store. As expected, the inviscid shock is too strong and too far aft compared to data, whereas the N-S solution results in a softened expansion and brings the aft-shock into better agreement with data. The quality of correlation for the N-S solution is marginal due to insufficient grid resolution around the store fins.

A typical N-S solution required 254MW of memory and 11 hours of CRAY C90 time. With a multitasking efficiency of 6 out of 10 processors, each case was completed in 2 wallclock hours.

3.2.5 HSR Cruise– N-S, Supersonic, Aeroelastic

Ref. [37] presents a simple technique that accounts for aeroelastic deformations experienced by High-Speed Research (HSR) wind-tunnel models within CFD computations. During wind-tunnel tests of the low aspect-ratio planforms characteristic of HSR configurations (Fig. 12), the load induced displacement and twist of the thin outer wing panels tends to
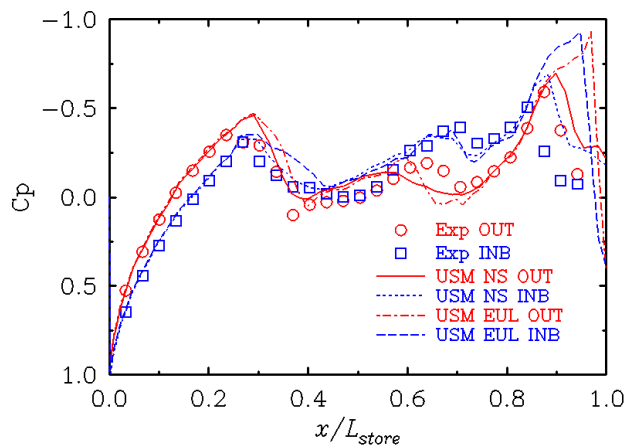

Fig. 11 Longitudinal distribution of surface pressure coefficient on F-16 generic finned-store body at Mach 0.95 and α=4 degrees. Store nose at x/L_{store}=0, and x/L_{store}=1 slightly aft of store fins.
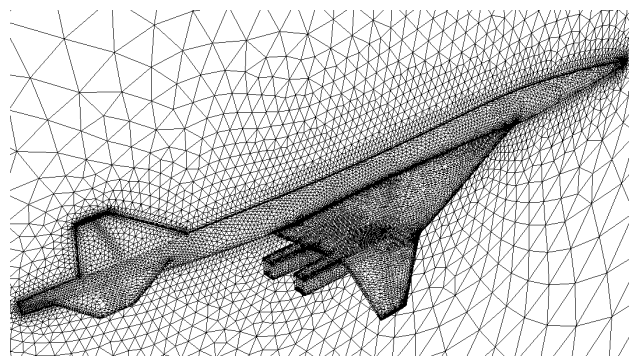

Fig. 12 Viscous tetrahedral grid on complete HSR configuration, 1,428,427 cells. Note thin-layer clustering on symmetry plane

unload those panels. This results in a decrease in lift and increase in pitching moment. The variation of drag with lift is not adversely affected. Thus, it is important to include the model deformation within numerical simulations to remove the noted aeroelastic-induced inconsistencies.

The USM3Dns N-S grid and solution is coupled with the ELAPS code within the modular TetrUSS framework. The ELAPS model is calibrated against the static bending characteristics of the wind-tunnel model in a manner similar to that described in Sec. 3.2.1. At the time of this work, the viscous grid movement described in Sec. 2.1.3 had not been automated and was accomplished manually through POSTGRID.

Fig. 13 depicts the CFD correlations with experimental force and moment data at M_∞=2.4 and Re_{cref}=6.4 million. Note that the USM3Dns result for the 'rigid' geometry over-predicts lift and significantly under-predicts pitching moment. The drag coefficient is in good agreement and includes corrections for nacelle base pressure and for trip drag.

The ELAPS calibration point is denoted by the *solid* triangle on the pitching-moment curve. The remaining *open* triangles were computed with USM3Dns using the calibrated ELAPS model. Note the good agreement of both the lift curve and the pitching moment across the range of experimental data. Note further the excellent agreement with the CFL3D computation [38]. The CFL3D result was computed on a deformed *structured* grid that matched the *optically measured* shape of the wind tunnel model.

4   Status of Emerging Capability

The following contains a brief synopsis of published work that is currently underway. These capabilities are not presently in the *TetrUSS* system.

4.1   Solution Adaptive Grids

Solution adaptive grid technology is a powerful tool in CFD that provides three main benefits for solving complex aerodynamic problems:
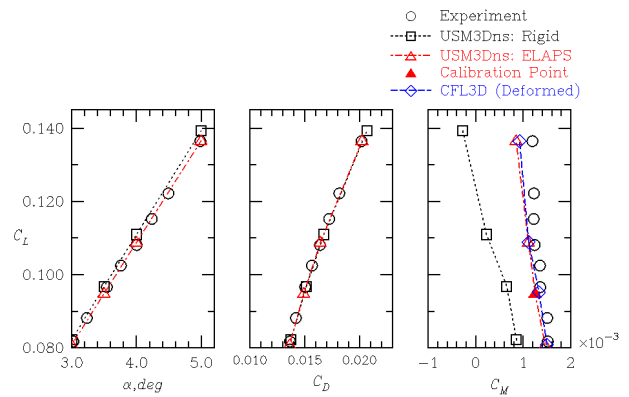

Fig. 13 Effect of calibrated USM3Dns/ELAPS on force and moment correlation for HSR configuration. Mach=2.4, Re_c=6.4 million.

increased automation, better solution accuracy, and computational efficiency. An adaptive unstructured grid refinement technique has been developed and applied successfully to three-dimensional inviscid flow test cases [39]. The method is based on a combination of grid subdivision and local remeshing. With this approach, the surface triangulation is first "h-refined" locally, and the tetrahedral grid in the field is then partially remeshed at locations of dominant flow features. The grid movement technique, described in an earlier section of this paper, is also incorporated in the present adaptive grid package for geometric adaptation of volume grids to moving or deforming surfaces.

4.2   Advanced Turbulence Models

Two advanced turbulence models have been implemented into a working version of USM3Dns [40] and are currently being tested. The models are based on modified versions of the original Jones and Launder k-ε two-equation turbulence model [41] and the Girimaji algebraic Reynolds stress model [42]. The current one-equation S-A model has shortcomings in predicting large-scale separated flows and shear flow. This work is motivated by the need for better predictions of those phenomena and to establish the code framework for investigating other two-equation models.

5   Concluding Remarks

TetrUSS is a synthesis of key state-of-the-art *unstructured*-grid technologies into a loosely coupled software system to form a user-friendly aerodynamic analysis and design tool. Salient features and capabilities include:

- The interactive GridTool code provides a key bridge between CAD surface definitions and the VGRIDns grid generator.

- The VGRIDns code is an established computer program for automatic generation of tetrahedral *unstructured* grids. It produces thin-layered tetrahedra suitable for computing Navier-Stokes flow solutions, and high-quality anisotropically stretched tetrahedral cells that dramatically reduce the overall grid size without compromising solution accuracy. A robust 'viscous' grid movement capability is also available.

- USM3Dns produces efficient and accurate Euler and Navier-Stokes flow solutions on vector processors and massively parallel computers. The Spalart-Allmaras one-equation turbulence model is presently utilized and is routinely coupled with a wall function. Special boundary conditions are provided for wake flow, jet engine simulation, and propellers. A low-Mach number preconditioning version is available.

- Modular engineering capabilities are provided for low-cost Euler/IBL viscous analysis, iterative design using the CDISC code, and static aeroelasticity.

- Several supportive utility codes are available under a single interface.

In summary, *TetrUSS* has enabled rapid solutions to many complex aerodynamic problems. Applied aerodynamicists from a broad cross-section of background and skill level have successfully applied the system to their tasks.

Work continues toward upgrading *TetrUSS* capabilities. The most near-term additions will be solution-adaptive grids, advanced two-equation turbulence models, and porting to PC clusters.

6   References

[1] Venkatakrishnan V. A perspective on unstructured grid flow solvers. NASA CR 195025, February 1995.

[2] Löhner R and Parikh P. Three-dimensional grid generation by the advancing front method. *Int.J.Num.Meth. Fluids* 8, pp 1135-1149 (1988).

[3] Pirzadeh S. Three-dimensional unstructured viscous grids by the advancing layers method. *AIAA Journal*, Vol. 34, No. 1, January 1996, pp. 43-49.

[4] Marcum D and Weatherill N. Unstructured Grid generation using iterative point insertion and local reconnection. *AIAA Journal*, 33, p. 1619, 1995.

[5] Löhner R. Generation of unstructured grids suitable for RANS calculations. AIAA Paper 99-3251, 1999.

[6] Hassan, O, Morgan K, Probert, E, and Peraire J. Unstructured tetrahedral mesh generation for three-dimensional viscous flows. *Int.J.Num.Meth. Engineering*, Vol. 39, pp 549-567, 1996.

[7] Samareh J. GridTool: A surface modeling and grid generation tool. *Proceedings of the Workshop on Surface Modeling, Grid Generation, and Related Issues in CFD Solutions*, NASA CP-3291, May 9-11, 1995.

[8] IGES: *Initial Graphics Exchange Specification* (IGES 5.3, 1996), U.S. Product Data Association, Charleston, SC, 1994.

[9] Pirzadeh S. Structured background grids for generation of unstructured grids by advancing front method. *AIAA Journal*, Vol. 31, No. 2, pp 257-265, February 1993.

[10] Pirzadeh S. Unstructured viscous grid generation by advancing-layers method. *AIAA Journal*, Vol. 32, No. 8, pp 1735-1737, August 1994.

[11] Frink N. Upwind scheme for solving the Euler equations on unstructured tetrahedral meshes. *AIAA Journal*, Vol., No. 1, pp 70-77, January 1992.

[12] Frink N. Tetrahedral unstructured Navier-Stokes method for turbulent flows. *AIAA Journal*, Vol. 36, No. 11, pp 1975-1982 November 1998.

[13] Roe P. Characteristic based schemes for the Euler equations. *Annual Review of Fluid Mechanics*, Vol. 18, pp 337-365, 1986.

[14] Frink, N. Recent progress toward a three-dimensional unstructured Navier-Stokes flow solver. AIAA 94-0061, January 1994.

[15] Anderson W and Bonhaus D. An implicit upwind algorithm for computing turbulent flows on unstructured grids. *Computers Fluids*, Vol. 23, No. 1, pp 1-21, 1994.

[16] Spalart P and Allmaras S. A one-equation turbulence model for aerodynamic flows. AIAA Paper 92-0439, January 1992.

[17] Frink N, Pirzadeh S and Parikh P. An unstructured-grid software system for solving complex

aerodynamic problems. NASA CP-3291, pp 289-308, May 9-11, 1995.

[18] Hartwich P and Frink N. Estimation of propulsion effects on transonic flows over a hypersonic configuration. AIAA Paper 92-0523, January 6-9, 1992.

[19] Pandya M, Bhat M and Parikh P. Application of unstructured grid methodology to rotorcraft flows. AHS-97, Presented at the *American Helicopter Society Rotorcraft Acoustics and Aerodynamics Specialists Meeting*, Williamsburg, Virginia, October 28-30, 1997.

[20] Bhat M and Parikh P. Parallel implementation of an unstructured grid-based Navier-Stokes solver. AIAA 99-0663, January 1999.

[21] Karypis G and Kumar V. Metis: A software package for partitioning unstructured graphs, partitioning meshes, and computing fill-reducing ordering of sparse matrices, version 3.0.3. University of Minnesota, November 1997.

[22] Pandya M. Low-speed preconditioning for an unstructured grid Navier-Stokes solver. AIAA 99-3134, June 1999.

[23] Weiss J and Smith W. Preconditioning applied to variable and constant density flows. *AIAA Journal*, Vol. 33, No. 11, pp 2050-2057, November 1995.

[24] Parikh P. Development of a modular aerodynamic design system based on unstructured grids. AIAA 97-0172, January 1997.

[25] Cavallo P. Coupling static aeroelastic predictions with an unstructured-grid Euler/interacting boundary layer method. Master's Thesis for The George Washington University, July 1995.

[26] Campbell R. Efficient viscous design of realistic aircraft configurations. AIAA 98-2539, June 1998.

[27] Smith W. Improved pressure and lift predictions in transonic flow using an unstructured mesh Euler method with an interacting boundary layer. Master's Thesis for The George Washington University, July 1994.

[28] Giles G. Further generalization of an equivalent plate representation for aircraft structural analysis. *Journal of Aircraft*, Vol. 26, pp 67-74, January 1989.

[29] Guruswamy G. User's guide for ENSAERO-A multidisciplinary program for fluid/structures/ control interaction studies of aircraft. NASA TM 108853, October 1994.

[30] Cebeci T, Clark R, Chang K, Halsey N and Lee K. Airfoils with separation and the resulting wakes. *Journal of Fluid Mechanics*, Vol. 163, pp 323-347, 1986.

[31] Green J, Weeks D and Brooman J. Prediction of turbulent boundary layers and wakes in compressible flow by a lag entrainment method. RAE Technical Report 72231, 1973.

[32] Parikh P, Pirzadeh S and Löhner R. A package for 3-D unstructured grid generation, finite-element flow solutions, and flow-field visualization. NASA CR-182090, September 1990.

[33] Hummel D. On the vortex formation over a slender wing at large angles of incidence. AGARD CP-247, *High Angle of Attack Aerodynamics, Paper No. 15,* January 1979.

[34] Krist S, Biedron R. and Rumsey C. CFL3D User's manual (version 5.0). NASA/TM-1998-208444, June 1998.

[35] Wai J, Herling W and Muilenburg D. Analysis of a joined-wing configuration. AIAA 94-0657, January 10-13, 1994.

[36] Frink N and Pirzadeh S. Tetrahedral finite-volume solutions to the Navier-Stokes equations on complex configurations. *Int. J. Numer. Meth. Fluids*, Vol. 31, pp 175-187, 1999. Also available as NASA/TM-1998-208961, December 1998,

[37] Frink N, Allison D and Parikh P. Unstructured Navier-Stokes analysis of wind-tunnel aeroelastic effects on TCA Model 2. *1999 NASA High-Speed Research Program Aerodynamic Performance Workshop*, NASA/CP-1999-209704, Volume 1, Part 1, pp 621-640, December 1999.

[38] Kuruvila G, Hartwich P and Baker M. The effect of aeroelasticity on the aerodynamic performance of the TCA. *1998 NASA High-Speed Research Program Aerodynamic Performance Workshop*, NASA/CP-1999-209692, Volume 1, Part 2, pp 1589-1648, December 1999.

[39] Pirzadeh S. A solution adaptive technique using tetrahedral unstructured grids. ICAS Paper No. 0262, presented at the *22nd International Congress of Aeronautical Sciences*, Harrogate United Kingdom, Aug. 27-Sept. 1, 2000.

[40] Wang, Q, Massey S, Abdol-Hamid K and Frink N. Solving Navier-Stokes equations with advanced turbulence models on three-dimensional unstructured grids. AIAA 99-1056, January 1999

[41] Jones W and Launder B. The prediction of laminarization with a two-equation model of turbulence. *Int. J. Heat Mass Transf.*, Vol. 15, pp 301-314, 1972.

[42] Girimaji S. Fully-explicit and self-consistent algebraic Reynolds stress model. NASA CR-198243, 1995